

Imaging Artifacts and Segmentation Errors With Wide-Field Swept-Source Optical Coherence Tomography Angiography in Diabetic Retinopathy

Ying Cui^{1,2,*}, Ying Zhu^{1,3,*}, Jay C. Wang¹, Yifan Lu⁴, Rebecca Zeng^{1,5}, Raviv Katz¹, David M. Wu¹, Demetrios G. Vavvas¹, Deeba Husain¹, Joan W. Miller¹, Leo A. Kim¹, and John B. Miller¹

¹ Retina Service, Massachusetts Eye and Ear, Department of Ophthalmology, Harvard Medical School, Boston, MA, USA

² Guangdong Eye Institute, Department of Ophthalmology, Guangdong Provincial People's Hospital, Guangdong Academy of Medical Sciences, Guangzhou, China

³ Department of Ophthalmology, Xiangya Hospital, Central South University, Changsha, Hunan, China

⁴ Harvard Medical School, Boston, MA, USA

⁵ Boston University School of Medicine, Boston, MA, USA

Correspondence: John B. Miller, Retina Service, Mass. Eye and Ear, Harvard Medical School, 243 Charles St, Boston, MA 02114, USA. e-mail: john_miller@meei.harvard.edu

Received: 9 July 2019

Accepted: 19 September 2019

Published: 15 November 2019

Keywords: artifact; segmentation error; optical coherence tomography angiography; wide field; diabetic retinopathy

Citation: Cui Y, Zhu Y, Wang JC, Lu Y, Zeng R, Katz R, Wu DM, Vavvas DG, Husain D, Miller JW, Kim LA, Miller JB. Imaging artifacts and segmentation errors with wide field swept source optical coherence tomography angiography in diabetic retinopathy. *Trans Vis Sci Tech.* 2019;8(6):18, <https://doi.org/10.1167/tvst.8.6.18>
Copyright 2019 The Authors

Purpose: To analyze imaging artifacts and segmentation errors with wide-field swept-source optical coherence tomography angiography (SS-OCTA) in diabetic retinopathy (DR).

Methods: We conducted a prospective, observational study at Massachusetts Eye and Ear from December 2018 to March 2019. Proliferative diabetic retinopathy (PDR), nonproliferative diabetic retinopathy (NPDR), diabetic patients with no diabetic retinopathy (DR), and healthy control eyes were included. All patients were imaged with a SS-OCTA and the Montage Angio (15 × 9 mm) was used for analysis. Images were independently evaluated by two graders using the motion artifact score (MAS). All statistical analyses were performed using SPSS 25.0 and R software.

Results: One hundred thirty-six eyes in 98 participants with the montage image were included in the study. Patients with more severe stages of DR had higher MAS by trend test analysis ($P < 0.05$). The occurrence of segmentation error was 0% in the healthy group, 10.53% in the no DR group, 10.00% in the NPDR group, and 50% in the PDR group. Multivariate regression analysis showed that the severity of DR and dry eye were the major factors affecting MAS ($P < 0.05$). There were some modifiable artifacts that could be corrected to improve image quality.

Conclusions: Wide field SS-OCTA assesses retinal microvascular changes by noninvasive techniques, yet distinguishing real alterations from artifacts is paramount to accurate interpretations. DR severity and dry eye correlated with MAS.

Translational Relevance: Understanding contributing factors and methods to reduce artifacts is critical to routine use and clinical trial with wide-field SS-OCTA.

Introduction

As optical coherence tomography angiography (OCTA) becomes more widely available in clinical practice, it is important to understand the advantages and limitations of this emerging modality.¹ The vascular changes of diabetic retinopathy (DR) have been well characterized with OCTA.² OCTA has the

advantage of resolving more structural details of many microvascular abnormalities than fluorescein angiography (FA), such as the foveal avascular zone (FAZ) enlargement and irregularity, capillary non-perfusion, intraretinal microvascular abnormalities (IRMA), and preretinal neovascularization (NV).^{3,4} Furthermore, OCTA can separately detect the superficial capillary and the deep capillary plexus (DCP)

that generally are overlaid and seem fused in standard angiographies.⁵ With the advent of wide-field swept-source OCTA (SS-OCTA), OCTA shows the potential to replace FA in the diagnosis and monitoring of DR.^{6–8}

However, imaging artifacts remain common in OCTA, which can lead to inaccuracies and limit its utility.⁹ Assessing the quality of OCTA images is essential when using OCTA for the diagnosis and monitoring of DR. Artifacts can arise from poor patient cooperation, media opacity, optical aberrations, and machine-related segmentation errors. It is of great importance to analyze and understand motion artifacts and segmentation errors before performing further qualitative and quantitative analysis with OCTA images. However, few studies^{9–11} on artifacts and segmentation errors have been carried out, especially in DR using wide-field SS-OCTA.

The aim of our study was to specifically evaluate wide-field SS-OCTA image quality, artifacts, and segmentation errors in DR, as well as to investigate the major factors affecting image quality. In addition, we share our experience using wide field SS-OCTA and experiences to maximize image quality and minimize image artifacts.

Methods

Subjects

We conducted a prospective, observational study at Massachusetts Eye and Ear (MEE) from December 2018 to March 2019. Proliferative DR (PDR), non-proliferative DR (NPDR), diabetic patients with no DR, and healthy control eyes with no ocular diseases were included. Exclusion criteria included eyes with concomitant retinal diseases, severe media opacities, signal strength index (SSI) less than seven using the default settings of the instrument, and low image quality preventing creation of a montage image automatically by the device. This study was approved by the institutional review board of MEE and informed consent was obtained from all subjects. All procedures adhered to the tenets of the Declaration of Helsinki and Health Insurance Portability and Accountability Act regulations.

Swept-Source OCTA

For each visit, all participants underwent ophthalmic examination, including Snellen best-corrected visual acuity (BCVA), slit-lamp examination, intraocular pressure, and dilated fundus examination. All

subjects were imaged with a 100-kHz SS-OCTA instrument (Plex Elite 9000; Carl Zeiss Meditec Inc., Dublin, CA) that uses a laser at a central wavelength of 1060 nm with a bandwidth of 100 nm.¹² We used the Montage Angio (15 mm × 9 mm; 2-scan composite) as the primary scan protocol. The montage image was obtained by combining separate superior and inferior 15 × 9-mm scans into a single image with a field of view (FOV) greater than 50° centered on the fovea. The Angio 15 × 9-mm scans used 500 A-scans per B-scan, resulting in an A- and B-scan separation of 24 μm. After a quality check 15 × 9-mm images were montaged using the automatic montage export function available on the device.

Vascular layers were segmented automatically using the built-in custom segmentation of the device. The vitreoretinal interface (VRI) slab was defined with an inner boundary of 300 μm above the internal limiting membrane (ILM) and an outer boundary of 30 μm below the ILM. The superficial capillary plexus (SCP) extended from the ILM to the inner plexiform layer (IPL), and the DCP from the IPL to the outer plexiform layer (OPL). The choriocapillaris (CC) extended from 29 μm beneath the retinal pigment epithelium (RPE) to 49 μm beneath the RPE, and the choroidal layer had a thickness of 51 μm and extended from 64 to 115 μm below Bruch's membrane.¹³ The different layers were color-coded as follows: VRI as purple, SCP as red, and DCP as green.

Evaluation for Artifacts and Segmentation Errors

The classification and detailed definition for artifacts^{9,14} in montage OCTA images were summarized in Table 1. The motion artifact score (MAS) is a grading system used to quantify motion artifact. The grading criterion for MAS was based on a previous study¹⁰ and revised according to the characteristics of montage images (Table 2). A higher MAS reflects more artifacts and lower image quality. Motion artifacts caused by eye movement or software correction of eye movement (stretching, displacement, vessel doubling) were all included in MAS to systematically evaluate image quality. The SCP was used for the evaluation of MAS because it included the large landmark vessels of the superficial plexus and was free from projection artifacts. Due to signal loss in the periphery of the image, only the area within 7 mm of the fovea was evaluated. Demographic data, clinical data regarding diabetes, as well as dry eye

Table 1. Classification and Definition of Artifacts in OCTA Montage Images

Classification	Artifacts	Definition
Systemic artifacts	Projection artifact	Vascular structures of superficial layers were mistakenly shown in deeper layers.
	Masking	Media opacity or certain lesions (e.g., macular edema, PED) caused signal loss in underlying layers.
	Unmasking	Signal loss in certain areas (e.g., retinal or RPE atrophy) lead to signal enhancement in underlying layers.
	Loss of signal	Appeared as a localized area of signal loss on the en face image due to loss of scan focus, more common in eyes with tumor, high myopia, or hyperopia, partially operator-dependent.
Image processing and display (depend on the type of device)	Segmentation artifact	A deviation of the certain slab caused by errors in (automatic) segmentation.
	Duplication of vessels	Defined as two copies of each blood vessel in the en face image caused by software correction of eye motion.
	Alignment error	The superior and inferior part of the montage image appeared to be of different depth, possibly due to projection removal
Artifacts caused by movement	Displacement	Very thin vertical lines leading to an apparent interruption or displacement of the vessels caused by eye movements.
	Blink artifact	A region of lost image information related to eye movement. It appears as an end-to-end black line of varying width through all depths of en face scans.
	Stretch artifact	Short strips of different brightness at the edge of OCTA shots.

diagnoses derived from medical records influencing patients' fixation ability were taken into consideration as possible factors related to image quality in regression analysis.

The occurrence of segmentation errors in all layers was evaluated for each montage image. If segmentation deviated from the correct plane by more than 50 μm , it was defined as inaccurate.¹⁵ Segmentation errors due to artifacts were excluded from the evaluation of segmentation accuracy.

The machine provided a default SSI for each image, which was used as an initial evaluation of image quality.

Wide-field OCTA images were independently evaluated for the artifacts and segmentation errors by two independent experienced ophthalmologists (YC and YZ), at different timepoints and in different orders. A third trained grader (JBM) adjudicated in cases of discrepancy. All images were evaluated on the instrument display screen in a standardized, dimmed environment.

Statistical Analysis

Statistical analyses were performed using SPSS version 25.0 (IBM Corporation, Somers, NY, USA)

and R software (the R Foundation for Statistical Computing, Vienna, Austria). Normally distributed continuous variables were presented as mean \pm standard deviation, and nonnormally distributed continuous data were presented as median (interquartile range [IQR]). Differences between groups were compared using mixed-model analysis (normally distributed variables) or Clustered Wilcoxon rank sum test (nonnormally distributed variables), as appropriate. Trend test analysis was used to assess the association between the severity of DR and MAS. Considering the inclusion of both eyes of the same participants, univariable and multilevel mixed-effect linear models were performed to determine clinical factors associated with SSI of OCTA images. Intergrader reproducibility was assessed by Cohen's kappa coefficient. A 2-tailed *P* value of less than 0.05 was considered statistically significant for all analysis.

Results

Demographic Data

One hundred thirty-six eyes (48 eyes with PDR, 40 eyes with NPDR, 19 eyes of diabetic patients without

Table 2. Revised SS-OCTA MAS (Score 1–6)

Score	Definition
1	No or slight displacement, absence of all other artifacts due to motion or software correction
2	Slight or moderate displacement, nonsignificant black line
3	Significant displacement, vessel doubling, stretch artifacts or nonsignificant black line in one quadrant
4	Significant displacement, vessel doubling, stretch artifacts, or nonsignificant black line in two quadrants
5	Significant displacement, vessel doubling, stretch artifacts, or significant black line in one quadrant
6	Significant displacement, vessel doubling, or stretch artifacts or significant black line in two quadrants

DR, and 29 healthy eyes) in 98 participants with montage images were included in the study (Table 3). The average age of the participants was 55.49 ± 13.77 years, and there was no significant difference in age among the four groups ($P = 0.759$). Seventy-one patients with DM were included, of which 13 (18.3%) had type 1 diabetes mellitus (T1DM). Median logMAR BCVA was 0.04 (0, 0.18), with the worst being 0.70 (20/100 Snellen equivalent) in a PDR patient.

Characteristics of Artifacts in Montage Images

Representative images of artifacts in montage images with corresponding MAS are shown in Figure 1. The Angio 15×9 -mm image was composed of vertical scans from top to bottom, so the motion artifacts caused by eye movement were vertical. Alignment error, an artifact specific to montage images, arises from image processing. It only occurs in the retinal-depth encoded image with superior and inferior parts of the montage image appearing to be of different depth, possibly due to projection removal (Fig. 2). In our study, alignment error was observed in 18 eyes (13.24%) in montage 15×9 -mm Angio image after removing projection and no statistical difference was detected across groups ($P = 0.293$).

Table 3. Demographic Data of Participants

Parameter	Value
Participants (eyes)	98 (136)
Age, y mean \pm SD	55.49 ± 13.77
Sex (participants), <i>n</i> (%)	
Male	47 (48.0)
Female	51 (52.0)
Type of diabetes (participants) ^a	71
T1DM, <i>n</i> (%)	13 (18.3)
T2DM, <i>n</i> (%)	58 (81.7)
Duration of diabetes (years) ^a , <i>n</i> (IQR)	16.0 (10.0, 27.0)
HbA1c, % ^a , mean \pm SD	8.07 ± 1.74
Groups (severity of DR, eyes), <i>n</i> (%)	
Healthy eye	29 (21.3)
No DR in DM patients	19 (14.0)
NPDR	40 (29.4)
PDR	48 (35.3)
Involved eye, <i>n</i> (%)	
Right	74 (54.4)
Left	62 (45.6)
BCVA (LogMAR), <i>n</i> (IQR)	0.04 (0, 0.18)
Dry eye (eyes), <i>n</i> (%)	15 (11.0)

HbA1c, glycosylated hemoglobin.

^a All healthy participants were excluded from the statistical analysis of diabetes related parameters (e.g., duration of diabetes, HbA1c).

SSI, MAS, and Segmentation Errors in Montage OCTA Images

SSI and MAS across different groups were summarized in Table 4. There were statistically significant differences in SSI and MAS between healthy, no DR, NPDR, and PDR groups ($P < 0.001$). Patients with higher severity of DR had a significantly higher MAS ($P < 0.05$, trend test analysis). Compared with the superior part of the image, MAS in the inferior part was significantly higher in each group ($P < 0.05$). The quality of Angio image 15×9 mm in the inferior part was worse than that in the superior part.

Segmentation errors were absent in healthy eyes and occurred in 10.53% eyes of no DR group and 10.00% eyes of NPDR group. The highest occurrence of segmentation errors was in the inferior part in eyes of PDR group (50.0%). Segmentation errors were mostly observed in DR patients with NV, epiretinal membrane (ERM), diabetic macular edema (DME), and pigment epithelium detachment (PED). ILM and IPL were the segmentation boundaries most prone to

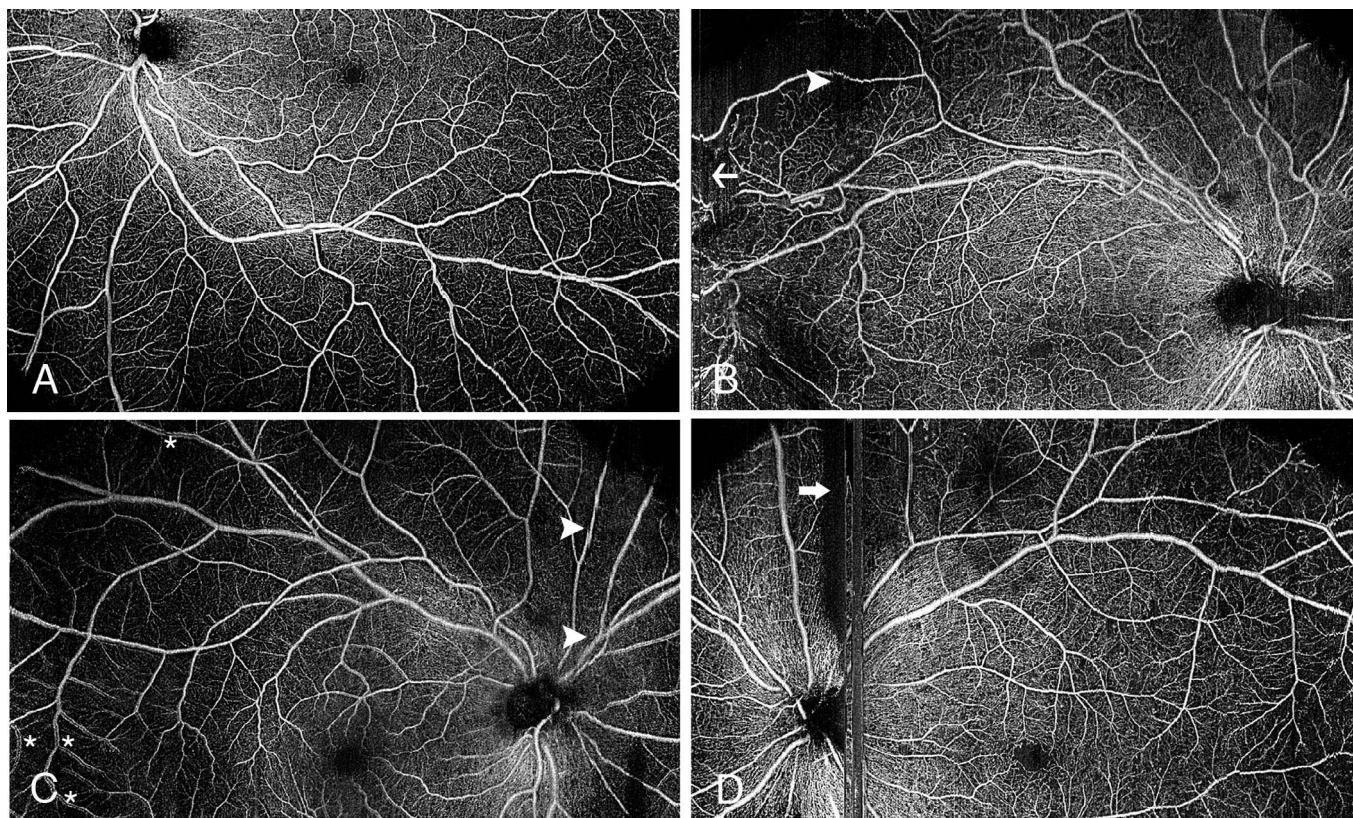


Figure 1. Representative images for MAS Grading. (A) MAS 1 with no obvious artifacts. (B) MAS 3 with significant displacement (*arrow head*) and nonsignificant black lines (*narrow arrow*) in one quadrant. (C) MAS 4 with significant displacement (*arrow head*) and vessel doubling (*) in two quadrants, no significant black lines. (D) MAS 5 with significant black lines (*wide arrow*) in one quadrant.

segmentation errors in all DR patients compared with the OPL and RPE (Fig. 3).

For interobserver reproducibility, we chose the MAS of the superior part in the NPDR group as the primary parameter to test. The MAS evaluated by two graders was 2.75 ± 1.50 and 2.80 ± 1.55 , respectively by paired sample *t*-test ($P = 0.481$). The concordance correlation coefficient was 0.996 ($P < 0.01$).

Factors Related to Image Quality

Univariate and multivariate regression analysis revealed that eyes with more severe stage of DR or older age had lower SSI ($P < 0.05$) (Table 5). Furthermore, eyes with more severe stages of DR or dry eye had higher MAS ($P < 0.05$) (Table 6).

However, there were also some factors (e.g., the size of pupil, head position of the examinee, adjustment of focus) that could be corrected to reduce modifiable artifacts. Figure 3 showed OCTA images of the PDR patient in two visits. Images taken with a small pupil had more artifacts in the second visit.

Though the young patient cooperated well, more artifacts, especially in the periphery were observed compared with the first visit. In Figure 4, a comparison of image quality before and after head position adjustment were displayed.

Discussion

The present study focused on the analysis of motion artifacts and segmentation errors in wide-field OCTA images of diabetic patients. We listed common motion artifacts and described alignment error (an artifact specific to montage images) in detail. We found that patients with higher severity of DR had a higher MAS and segmentation errors were more frequent in eyes with PDR. Because wide-field SS-OCTA has been used in the diagnosis and follow-up of DR,^{2,7,8,12,16} it is necessary to understand the factors that contribute to both segmentation and motion artifacts of montage images in order to ensure meaningful and reliable results. This is particularly important to accurately incorporate wide-field OCTA

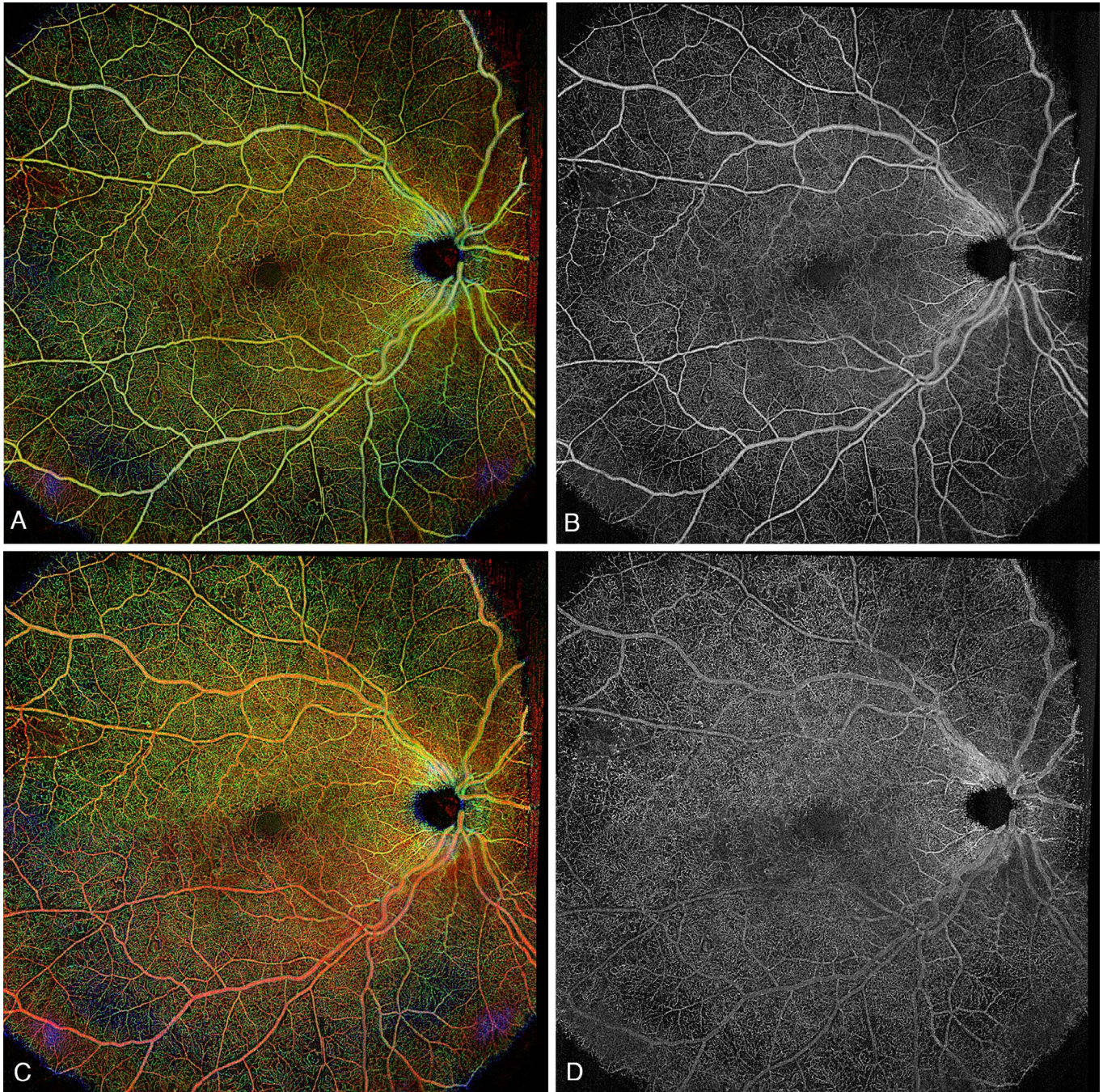


Figure 2. Alignment error. Both retinal-depth encoded (A, C) and DCP (B, D) montage images before (A, B) and after projection removal (C, D) are shown here. After projection removal, the upper and lower part of retinal-depth encoded montage image (C) appeared to be of different depth, which was defined as “alignment error.”

into our clinical decision making in DR patients as we examine small, quantitative differences in NV and nonperfusion areas.

This study was the first to describe artifacts and segmentation errors in wide-field SS-OCTA. Compared with conventional 6×6 -mm images, capturing the Angio 15×9 -mm image involves several of the

following additional considerations: (1) due to the longer acquisition time, fixation loss occurs more frequently resulting in more artifacts, especially in the periphery; (2) the curvature of the eye makes it difficult to keep in focus the long 15-mm scan span for the montage image throughout acquisition so loss of signal is more frequent than conventional, shorter

Table 4. SSI and MAS In Different Groups

Groups (Eyes)	Healthy (29)	No DR (19)	NPDR (40)	PDR (48)	<i>P</i> Value
Age	53.14 ± 13.17	55.58 ± 10.90	56.65 ± 15.89	54.50 ± 13.64	0.759
BCVA, median (IQR)	0 (−0.05, 0.05)	0.04 (0, 0.14)	0.02 (0, 0.18)	0.14 (0.04, 0.22)	<0.001
SSI, mean ± SD					
Superior	8.79 ± 0.49	9.00 ± 0.58	8.68 ± 0.76	8.44 ± 0.77	0.017
Inferior	8.76 ± 0.64	9.05 ± 0.62	8.55 ± 0.64	8.33 ± 0.78	0.001
Average	8.78 ± 0.51	9.03 ± 0.51	8.61 ± 0.57	8.39 ± 0.72	0.001
MAS, mean ± SD					
Superior	1.48 ± 0.69	1.89 ± 0.74	2.78 ± 1.54	3.02 ± 1.73	<0.001
Inferior	1.79 ± 1.01	2.11 ± 1.94	2.80 ± 1.62	3.40 ± 1.35	<0.001
Average	1.64 ± 0.71	1.97 ± 1.08	2.79 ± 1.40	3.21 ± 1.35	<0.001

scans; and (3) the Angio 15 × 9-mm image was composed of vertical scans from top to bottom, so the motion artifacts caused by eye movement were vertical.

We chose the montage 15 × 9-mm angio image as the scanning protocol for the following reasons: (1) most vascular abnormalities due to DR were located around the vascular arcades, which are easily captured by the montage images, and are more comparable to conventional FA, and (2) compared with montage (12 × 12 mm; 5-scan composite) Angio images, our scan protocol requires less exam time and better patient cooperation, which translates to fewer artifacts. Though the montage 12 × 12-mm angio images could provide more information about the nasal periphery, a previous study showed that DR vascular abnormalities were more frequent in the temporal fields compared with the nasal fields ($P < 0.0001$).¹⁷

The OCTA images with higher MAS score limited the ability to visualize fine capillary vessels and DR features. It may be difficult to grade DR severity level and figure out the boundary of nonperfusion area with MAS score of in Montage 15 × 9-mm OCTA image with MAS score of five and six. There are several artifacts assessed in this study, some of which have been previously described, especially systematic artifacts and artifacts caused by movement.^{10,14,18} However, the key point of the current study was to focus on artifacts in DR, in which we found a significant correlation between MAS and DR severity as well as dry eye in multivariate regression analysis. People with diabetes are more prone to suffer from dry eye than those without diabetes.^{19,20} Dry eye could increase the patient's blink frequency significantly and interfere with image acquisition.²¹ The fact that BCVA was not correlated with MAS in

multivariate regression analysis might be due to the following factors: (1) BCVA is an important factor contributing to patients' fixation ability; however, there are also other factors we need to consider (e.g., fixation loss, dry eye and the age of patients). The longer scan time is a challenge for patient's attention and some patients tend to lose fixation when they are tired. It also magnifies the effect of abnormality in ocular surface because more blinking will prolong the scan time, which makes a vicious circle; (2) we excluded eyes with SSI less than seven using the default settings of the instrument, and low image quality preventing creation of a montage image automatically by the device. According to the results, the worst BCVA of our included eyes was 20/100. It is possible eyes with worse BCVA were excluded from our analysis due to poor image quality. When patients have relatively good BCVA, other factors impacting their fixation ability might play a more important role.

We found an interesting phenomenon that the inferior part of montage image had a higher MAS compared with the superior part. We suppose it might be related to the following: (1) the default setting of the machine performing montage image scan was to do the superior Angio 15 × 9-mm scan first and the inferior Angio 15 × 9-mm scan after. It is not rare to see patient cooperation become worse when doing the inferior part scan. We will do an analysis about the effect of scan order on artifacts in the future, and (2) it is well-recognized that blinking and eyelid dynamics play important roles in the distribution of tears. Tear film break-up in healthy subjects was typically inferior.²² In the long process of scanning, reduced and incomplete blinking along with increased tear film break-up may explain the worse imaging quality of the inferior part.

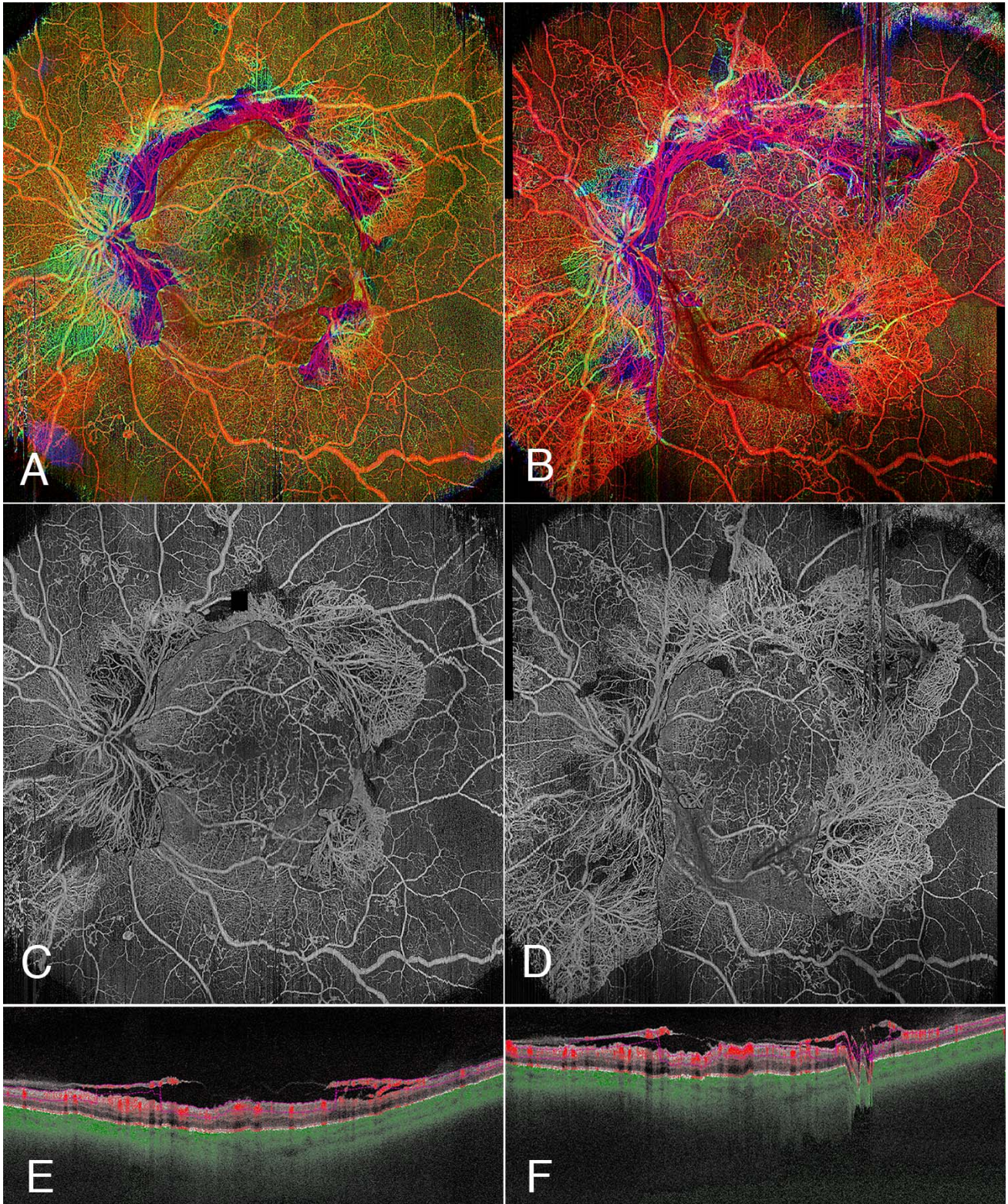


Figure 3. Representative OCTA images. Retinal-depth encoded (A, B), SCP (C, D), representative B scan showing segmentation error due to NV (E, F) for follow-ups of a PDR patient. The patient first presented with blurry vision 1 month after panretinal photocoagulation (A, C, E) and experienced significant progression at 1-month follow-up (B, D, F). The images at follow-up were taken with small pupil and had more artifacts compared with the first visit.

Table 5. Univariate and Multivariate Regression Analysis for SSI

Parameter	SSI Average (Univariate)		SSI Average (Multivariate)	
	B (95%CI)	P	B (95%CI)	P
Age (per 10 y)	-0.09 (-0.17, -0.02)	0.018	-0.09 (-0.16, -0.01)	0.019
DM duration (per 10 y)	-0.10 (-0.19, -0.01)	0.036		
BCVA, LogMAR	-0.77 (-1.54, -0.01)	0.048		
Severity of DR (groups)	-0.16 (-0.25, -0.07)	0.001	-0.15 (-0.24, -0.06)	0.001
DME	-0.30 (-0.54, -0.06)	0.014		
Dry eye	-0.48 (-0.82, -0.14)	0.006		

Furthermore, we described a montage-specific artifact “alignment error,” which was different from focus artifact described by Tomlinson et al.²³ It is related to image processing, in particular projection artifact removal. In fact, the retinal-depth encoded image could appear normal if one chose not to remove projection artifacts.

Incorrect segmentation results in anatomically incorrect en face OCTA images and consequently inaccurate quantification of vessel parameters in DR. Compared with conventional 6 × 6-mm images, the montage image covers a much larger area so any segmentation errors could also be magnified. In PDR patients, large areas of NV could lead to significant segmentation errors in the VRI and superficial retina slabs (Fig. 3), which often underestimated the size of the NV. DME can also cause segmentation errors in the DCP and interfere with the quantification analysis of vessel density. Fortunately, segmentation errors can be manually corrected by editing each segmentation line (ILM, IPL, OPL, RPE, RPE-fit) and then automatically propagating the changes, which applies the newly defined layer to all B-scans included in the scan. The correction of segmentation was critical to distinguish IRMA and NVE, which is of great value in the diagnosis of early PDR. Therefore, for DR patients with NV, ERM, DME, and PED, care

should be taken with segmentation errors and manual correction should be done accordingly to avoid misinterpretation of images.

One purpose of analyzing artifacts and segmentation errors was to identify ways to obtain higher quality images. Artifacts can be classified as unmodifiable and modifiable, and the latter was the focus for image-quality improvement. Though the use of eye-tracking technology could significantly decrease motion artifacts,²⁴ operator skill and patient cooperation still play an important role in obtaining a good image. This is especially true in wide-field OCTA because acquisition time is longer than conventional OCTA scans. Before imaging a patient, systemic and ocular evaluation should be performed to prepare the operator for possible difficulties. Patients with ocular conditions (e.g., nystagmus, ptosis, media opacity²⁵) and some systemic diseases (e.g., Parkinson’s disease, multiple sclerosis²⁶) could substantially undermine image qualities.

We suggest the following tips to help reduce modifiable artifacts with the wide-field SS-OCTA system used in the present study: (1) focus should be constantly adjusted to make good visibility of the retinal blood vessels sharp and clear during the long scan. We can use manual adjustment when the patient is not well positioned, with hyperopia or high myopia;

Table 6. Univariate and Multivariate Regression Analysis for MAS

Parameter	MAS Total (Univariate)		MAS Total (Multivariate)	
	B (95%CI)	P	B (95%CI)	P
Age (per 10 y)	0.17 (0.01, 0.34)	0.041	0.07 (-0.09, 0.23)	0.412
Sex (male vs. female)	0.11 (-0.35, 0.57)	0.645	0.05 (-0.36, 0.46)	0.804
DM duration (>12 years vs. ≤12)	0.60 (0.12, 1.09)	0.015		
BCVA, LogMAR	2.70 (1.10, 4.29)	0.001	1.29 (-0.32, 2.90)	0.115
Severity of DR (groups)	0.54 (0.36, 0.72)	<0.001	0.42 (0.22, 0.61)	<0.001
DME	0.86 (0.36, 1.36)	0.001		
Dry eye (yes vs. no)	1.45 (0.75, 2.14)	<0.001	1.07 (0.40, 1.75)	0.002

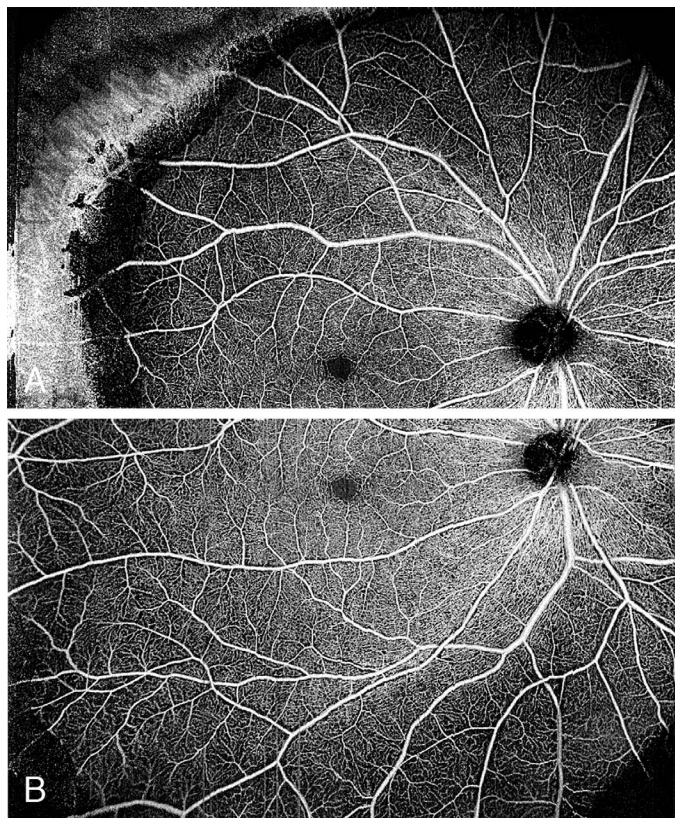


Figure 4. Representative OCTA images before (A) and after (B) head position adjustment. Once the chin or the forehead is not adhered to the machine, the image (A) will lose signal in the periphery and show artifacts. After head position adjustment, the image (B) was free of artifacts.

(2) keep head position stable is an essential way to avoid the motion artifacts; (3) it is possible to ask the patient to rotate the eye or adjust the eye alignment subtly by moving the chinrest settings to reduce the effect of small areas of vitreous opacity on image quality; and (4) dilation, using fixation light, rest between scans, blink during the scan and application of artificial tears are also helpful to get better OCTA images.

The present study is the first to investigate artifacts in wide-field SS-OCTA and provide some experience in obtaining higher quality montage images in DR patients. Some limitations of this study include the following: (1) though we described some systemic artifacts (projection artifacts, masking, unmasking, and loss of signal), image processing artifacts, they were not included in the statistical analysis for image quality; (2) the ocular surface condition was not evaluated with objective investigations and all dry eye diagnoses were derived from medical records; (3) the lens status was not included in the correlation

analysis; and (4) acquisition time of Angio 15 × 9-mm image was not evaluated.

In conclusion, both motion artifacts and segmentation errors are frequent in eyes with PDR using wide-field OCTA. It is necessary to assess these image artifacts in montage images in order to obtain meaningful and reliable results, especially in DR patients with DME, NV, PED, or ERM. As OCTA and wider scanning patterns become more common in DR clinical trials, identifying methods to improve image quality and reduce artifacts will be required to maximize the clinical application of this evolving, yet insightful OCTA technology.

Acknowledgments

Supported by Lions Clubs International Foundation Grant 530125.

Parts of this manuscript were presented at the ARVO imaging conference, 2019 in Vancouver, BC.

Disclosure: **Y. Cui**, None; **Y. Zhu**, None; **J.C. Wang**, None; **Y. Lu**, None; **R. Zeng**, None; **R. Katz**, None; **D.M. Wu**, None; **D.G. Vavvas**, None; **D. Husain**, None; **J.W. Miller**, Sunovion (C), KalVista Pharmaceuticals (C), ONL Therapeutics (C, P, I), Valeant Pharmaceuticals/Mass. Eye and Ear (P, R), Lowy Medical Research Institute (F); **L.A. Kim**, None; **J.B. Miller**, Carl Zeiss Meditec, Inc. (C); Heidelberg Engineering Inc. (C)

*Ying Cui and Ying Zhu contributed equally to this work.

References

1. Spaide RF, Fujimoto JG, Waheed NK, et al. Optical coherence tomography angiography. *Prog Retin Eye Res.* 2018;64:1–55.
2. Ting DSW, Tan GSW, Agrawal R, et al. Optical coherence tomographic angiography in type 2 diabetes and diabetic retinopathy. *JAMA Ophthalmol.* 2017;135:306–312.
3. Hwang TS, Jia Y, Gao SS, et al. Optical coherence tomography angiography features of diabetic retinopathy. *Retina.* 2015;35:2371–2376.
4. Savastano MC, Federici M, Falsini B, et al. Detecting papillary neovascularization in proliferative diabetic retinopathy using optical coherence tomography angiography. *Acta Ophthalmol.* 2018;96:321–323.

5. Savastano MC, Lumbroso B, Rispoli M. In vivo characterization of retinal vascularization morphology using optical coherence tomography angiography. *Retina*. 2015;35:2196–2203.
6. Chowdhary N, Shrivastav A, Koundanya VV, et al. Characteristics of neovascularization in early stages of proliferative diabetic retinopathy by optical coherence tomography angiography. *Am J Ophthalmol*. 2019;197:180.
7. Alibhai AY, De Pretto LR, Moulton EM, et al. Quantification of retinal capillary nonperfusion in diabetics using wide-field optical coherence tomography angiography [published online ahead of print December 18, 2018]. *Retina*. <https://doi.org/10.1097/IAE.0000000000002403>.
8. Russell JF, Shi Y, Hinkle JW, et al. Longitudinal wide-field swept-source OCT angiography of neovascularization in proliferative diabetic retinopathy after panretinal photocoagulation. *Ophthalmol Retina*. 2019;3:350–361.
9. Spaide RF, Fujimoto JG, Waheed NK. Image artifacts in optical coherence tomography angiography. *Retina*. 2015;35:2163–2180.
10. Lauermaun JL, Woetzel AK, Treder M, et al. Prevalences of segmentation errors and motion artifacts in OCT-angiography differ among retinal diseases. *Graefes Arch Clin Exp Ophthalmol*. 2018;256:1807–1816.
11. Say EAT, Ferenczy S, Magrath GN, et al. Image quality and artifacts on optical coherence tomography angiography: comparison of pathologic and paired fellow eyes in 65 patients with unilateral choroidal melanoma treated with plaque radiotherapy. *Retina*. 2017;37:1660–1673.
12. Zhang Q, Rezaei KA, Saraf SS, et al. Ultra-wide optical coherence tomography angiography in diabetic retinopathy. *Quant Imaging Med Surg*. 2018;8:743–753.
13. Gao SS, Jia Y, Zhang M, et al. Optical coherence tomography angiography. *Invest Ophthalmol Vis Sci*. 2016;57:OCT27–OCT36.
14. Lang GE, Enders C, Loidl M, et al. Accurate OCT-angiography interpretation - detection and exclusion of artifacts [in German]. *Klin Monbl Augenheilkd*. 2017;234:1109–1118.
15. Han IC, Jaffe GJ. Evaluation of artifacts associated with macular spectral-domain optical coherence tomography. *Ophthalmology*. 2010;117:1177–1189.e4.
16. You QS, Guo Y, Wang J, et al. Detection of clinically unsuspected retinal neovascularization with wide-field optical coherence tomography angiography [published online ahead of print March 4, 2019]. *Retina*. <https://doi.org/10.1097/IAE.0000000000002487>.
17. Silva PS, Cavallerano JD, Sun JK, et al. Peripheral lesions identified by mydriatic ultra-wide field imaging: distribution and potential impact on diabetic retinopathy severity. *Ophthalmology*. 2013;120:2587–2595.
18. Enders C, Lang GE, Dreyhaupt J, et al. Quantity and quality of image artifacts in optical coherence tomography angiography. *PLoS One*. 2019;14:e0210505.
19. Kaiserman I, Kaiserman N, Nakar S, et al. Dry eye in diabetic patients. *Am J Ophthalmol*. 2005;139:498–503.
20. Fuerst N, Langelier N, Massaro-Giordano M, et al. Tear osmolarity and dry eye symptoms in diabetics. *Clin Ophthalmol*. 2014;8:507–515.
21. Miura DL, Hazarbassanov RM, Yamasato CK, et al. Effect of a light-emitting timer device on the blink rate of non-dry eye individuals and dry eye patients. *Br J Ophthalmol*. 2013;97:965–967.
22. Himebaugh NL, Begley CG, Bradley A, et al. Blinking and tear break-up during four visual tasks. *Optom Vis Sci*. 2009;86:E106–E114.
23. Tomlinson A, Hasan B, Lujan BJ. Importance of focus in OCT angiography. *Ophthalmol Retina*. 2018;2:748–749.
24. Lauermaun JL, Treder M, Heiduschka P, et al. Impact of eye-tracking technology on OCT-angiography imaging quality in age-related macular degeneration. *Graefes Arch Clin Exp Ophthalmol*. 2017;255:1535–1542.
25. Konana VK, Shanmugam PM, Ramanjulu R, et al. Vitreous opacities causing artifacts in optical coherence tomography angiography. *Indian J Ophthalmol*. 2017;65:1023–1024.
26. Iftikhar M, Zafar S, Gonzalez N, et al. Image artifacts in optical coherence tomography angiography among patients with multiple sclerosis. *Curr Eye Res*. 2019;44:558–563.